Russian Journal of General Chemistry, Vol. 72, No. 4, 2002, pp. 622–631. Translated from Zhurnal Obshchei Khimii, Vol. 72, No. 4, 2002, pp. 667–677.

Electrosurface Characteristics of Element–Oxygen Nanostructures on Solid Supports

L. E. Ermakova, M. P. Sidorova, N. F. Bogdanova, and A. V. Klebanov

St. Petersburg State University, St. Petersburg, Russia

Received November 1, 2001

Abstract — Element (Si, Ti, Al, Sn, Fe)–oxygen nanostructures on supports of various nature (SiO_2, AlOOH) have been synthesized by molecular layering from the gas phase. The electrosurface characteristics (adsorption of potential-determining ions, electrokinetic potential, zero-charge point, isoelectric point) in solutions of 1–1 electrolytes have been determined for the objects synthesized. Conditions of molecular layering for preparing Al– and Sn–oxygen nanostructures with surface properties close to characteristics of the corresponding bulk oxides have been established.

In the colloid chemical literature, great attention is currently paid to the problem of formation and structure of the electrical double layer on oxide surfaces in electrolyte solutions. The interest in this problem is caused both by the wide occurrence of oxides in nature and their practical use and also by the increasing use of ultrathin (0.5–5 nm) oxide layers. Such two-dimensional layers on various solid supports are widely applied, in particular, in production of high-activity catalysts, ion-selective field transistors, a number of microelectronic devices, etc. [1–7]. It is of note that composition–structure–properties relationships for bulk (hydr)oxides and "thick" solid layers (more that 100 nm) is a well-explored topic, whereas ultrathin layers have scarcely been studied. The most thoroughly studied properties of such layers are their chemical composition and structural characteristics as functions of preparation method and conditions of further treatment [6–18]. However, there are only few studies [3, 19–21] of electrosurface properties of supported oxide nanolayers, although such properties determine technological parameters of the layers in many cases. For this reason, it was of interest to synthesize some element oxide nanostructures and to investigate their electrosurface characteristics. Investigation of the electrokinetic and adsorption properties of supported oxide nanolayers as a function of the degree of substitution of surface groups of the support and of the nanostructure thickness, and comparison of these properties with the characteristics of the corresponding bulk oxide would allow one to trace the transition from the characteristics of the support to the parameters of the deposited nanolayer and to find the minimum possible nanostructure thickness at which the support is completely shielded.

The method of molecular layering from the gas phase, developed by Aleskovskii and Koltsov [22, 23], is one of the most promising methods of synthesis of thin oxide layers on solid supports, since it allows preparation of solid substances of preset chemical composition and structure.

In this work, the synthesis of element–oxygen nanolayers on the surface of (hydr)oxide supports was performed in accordance with reactions (1) and (2) (on a silica support as example) [12–14, 24].

$$p(\equiv Si{-}OH) + ECl_m \longrightarrow (\equiv Si{-}O{-})_pECl_{m-p} + pHCl\uparrow, \quad (1)$$

$$E = Si, Al, Ti, Sn, Fe.$$

Upon treatment of the resulting product with water vapor, chlorine is replaced by hydroxy groups:

$$(\equiv Si{-}O{-})_pECl_{m-p} + (m - p)\ H_2O \longrightarrow (\equiv Si{-}O{-})_pE(OH)_{m-p} + (m - p)\ HCl\uparrow. \quad (2)$$

The presence of hydroxy groups in the reaction product makes possible the synthesis to be continued until the element–oxygen nanolayer attains the required thickness, by alternating reactions (1) and (2).

The choice of the temperature of the synthesis is determined by the decomposition onset temperature of surface functional groups. In the case of silanol surface groups, the synthesis of oxide nanolayers should be carried out at a temperature not higher than 180–200°C, since the hydroxyl cover of silica undergoes decomposition starting from that temperature.

It is also of note that the synthesis via reactions (1) and (2) should be used with those low-molecular re-

1070-3632/02/7204-0622 $27.00

agents which are capable of completely replacing hydroxyl protons of the support, such as chlorides of many elements, organoelement compounds, etc. If the substitution of OH by oxychloride groups (for example, reactions with $SnCl_4$, $GeCl_4$, WCl_6, etc.) occurs incompletely or is necessary to perform at temperatures above 200°C (for example, reactions with low-volatile chlorides, such as $FeCl_3$), when the number of OH groups is decreased by surface dehydration processes, it is advisable to use other initial functional groups, more heat-resistant, such as OCH_3 [10, 11].

With methoxy groups, the following surface reactions proceed in the course of the synthesis (with a silica support as example):

$$[SiO_2]_{k-1}O_2SiOH + CCl_4 \longrightarrow [SiO_2]_{k-1}O_2SiCl + COCl_2\uparrow + HCl\uparrow, \quad (3)$$

$$[SiO_2]_{k-1}O_2SiCl + CH_3OH \longrightarrow [SiO_2]_{k-1}O_2SiOCH_3 + HCl\uparrow, \quad (4)$$

$$m[SiO_2]_{k-1}O_2SiOCH_3 + ECl_j \longrightarrow [SiO_2]_{m(k-1)}(O_2Si{-}O{-})_mECl_{j-m} + mCH_3Cl\uparrow, \quad (5)$$

$$[SiO_2]_{m(k-1)}(O_2Si{-}O{-})_mECl_{j-m} + (j-m)H_2O \longrightarrow [SiO_2]_{m(k-1)}(O_2Si{-}O{-})_mE(OH)_{j-m} + (j-m)HCl\uparrow. \quad (6)$$

In this case, reactions (3) and (4) are used to form methoxy functional groups on the support surface, and the number of deposited element–oxygen monolayers is determined by the number of alternant reactions (5) and (6).

The samples were obtained using a setup (Fig. 1) that allowed molecular layering reactions to be performed in a flow of air dried with phosphorus oxide to a residual moisture of 2 mg/m^3. The dried air was saturated with vapor of silicon and titanium chlorides at 20°C, of stannum chloride at 20 and 100°C, of aluminium chloride at 200°C, and of iron chloride at 200 and 250°C, and fed to the reactor with a quartz plate or with a portion of powdered bulk (hydr)oxide (0.5 to 1 g). The synthesis of nanostructures in the reactor was performed at 200 and 250°C. After the hydrogen chloride formed by reaction (1) was replaced with dry air, the reaction product was treated with water vapor at 200°C until HCl no longer evolved and then dried in a flow of dry air at 200°C. Heating was perfomed with a Ni–Cr wire, and the temperature was measured with a thermocouple. The thickness of the oxide nanolayer on the support surface was determined by the number *n* of molecular layering cycles.

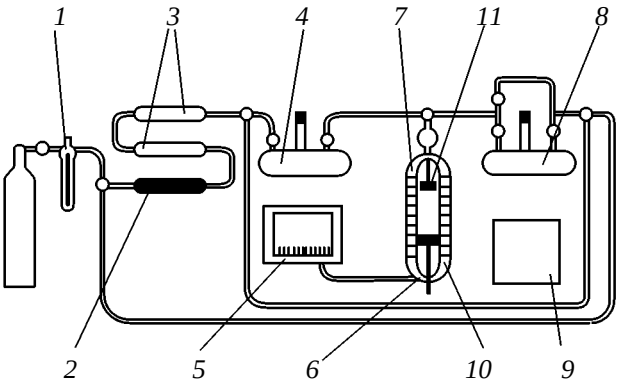

Fig. 1. Scheme of the setup for the synthesis of element–oxygen nanostructures on solid supports by molecular layering from the gas phase: (*1*) flowmeter, (*2*, *3*) dessicant for carrier gas, (*4*) gooseneck with reagent, (*5*) potentiometer, (*6*) thermocouple, (*7*) reactor, (*8*) gooseneck with water, (*9*) voltage controller, (*10*) support, (*11*) cup with solid chloride.

The chemical composition of the synthesized nanolayers was performed by treatment of samples with 2 N sulfuric acid with heating to dissolve the deposited element–oxygen layer. The contents of aluminium, tin, and iron in the solution were determined by photoelectrocolorimetry.

Since the isoelectric point (IEP) of the (hydr)oxide surface in solutions of potential-determining ions is, together with the zero-point charge (ZPC), is one of the most important characteristics of the surface, then, by comparing the pH_{IEP} values for bulk (hydr)oxides and thin element–oxygen layers, one can follow changes in the electrochemical properties of the support in the course of deposition. The change in the electrosurface characteristics of the modified surface will be more pronounced in the case when the isoelectric points of the support and the deposited oxide in the bulk are appreciably different. For this reason, for preparing Ti–, Fe–, and Al–oxygen nanolayers we chose various silica supports with pH_{IEP} = 2–3, while for Sn–oxygen nanolayers, aluminium hydroxide (AlOOH, boehmite), taking into account that for the latter $pH_{IEP} = pH_{ZPC} = 8.6 \pm 0.1$, whereas for tin(IV) oxide $pH_{IEP} = pH_{ZPC} = 4.0 \pm 0.1$ [25–29]. A quartz plane–parallel capillary, monodisperse spherical SiO_2 particles 0.5 μm in diameter, purchased from GelTech (hereinafter, these supports are labeled GT), Silochrom C-120, and Aerosil OX-50, and A-175 were used as silica supports. Before use Aerosil A-175 particles were treated with water vapor at 200°C and then dried at the same temperature (such surface is

below considered as initial). The synthesis of nanostructures was carried out both on the initial and on preliminary calcined (at 400–900°C) Aerosil A-175 surface. Preliminary thermal treatment led to partial dehydration of the surface, i.e. to the transformation of silanol groups into siloxane ones which do not take part in surface reactions. The degree of residual surface hydration is given by the ratio $\Theta = N^t_{OH}/N_{OH}$, where N_{OH} and N^t_{OH} are the surface concentrations of silanol groups on the initial and calcined surface, respectively. In the temperature range used, the Θ values varied from 0.1 to 1. At $\Theta < 1$, a mosaic surface structure appeared after the first cycle of molecular layering.

For the oxide structures synthesized, we measured (1) adsorption of potential-determining ions Γ_i ($i = H^+$, OH^-), by continuous potentiometric titration; (2) electrophoretic mobility U_{ef} of dispersed particles, by ultramicroelectrophoresis; and (3) streaming potential E_S for plane–parallel capillaries [25, 26]. The surface electrokinetic potential ζ of nanostructures was calculated by the following equations:

$$\zeta^S = \frac{\eta}{\varepsilon\varepsilon_0} U_{ef}, \quad (7)$$

$$\zeta = \eta æ E_S/\varepsilon\varepsilon_0 P, \quad (8)$$

where η is the viscosity of the liquid, ε and ε_0 are the dielectric permittivities of the medium and vacuum, respectively, æ is the conductivity of the solution in the plane–parallel capillary, and P is pressure. The ζ values calculated by Smoluchowski's equation (7) are supplied with the index S. The index W relates to the ζ values found with allowance for polarization of electrical double layer in terms of the Overbeek–Booth–Wiersema theory [30].

The electrosurface characteristics were measured within the pH range 3–9 on the background of 10^{-3}– M KCl and NaCl solutions at 20°C. Thus performed studies allowed us to compare the colloid-chemical properties of the synthesized element–oxygen nanostructures with the corresponding characteristics of the bulk silicon, aluminium, titanium, tin, and iron (hydr)oxides synthesized under conditions close to the conditions of the synthesis of nanostructures. Let us proceed to consideration of particular systems.

System nSiO$_2$/SiO$_2$

The investigation of the electrosurface characteristics of element–oxygen nanostructures we started with studying the electrokinetic properties of a model system, a quartz plane–parallel capillary (height 50 μm) covered with silicon–oxygen nanolayers. It was found earlier [16–18] that the properties of the first oxide layer deposited are cardinally different from those of bulk macrophase, and the increase of the number of layers to four leads to leveling of this difference. For this reason, to find out whether our synthetic conditions allow preparation of an oxide nanostructure with characteristics close to those of bulk oxide, we performed six cycles of molecular layering.

The measured electrokinetic potentials of the initial capillary and the capillary covered with an element–oxygen nanostructure are shown in Fig. 2 (curves *1* and *3*). Analysis of the ζ–pH dependence shows that the isoelectric point in HCl solutions ($pH_{IEP} = 3.0$) and the electrokinetic potentials of the initial support and the $6SiO_2/SiO_2$ surface practically coincide. Adding a background electrolyte (10^{-3} M NaCl), like with the initial capillary, decreases $|\zeta|$ values but has almost no effect on the isoelectric point [25].

Thus, the results obtained show that the deposition of a nanostructure of the same chemical composition as the support produce no changes in the principal electrokinetic surface characteristics: isoelectric point and ζ potential.

System nTiO$_2$/SiO$_2$

Titanium–oxygen nanostructures were synthesized on four SiO_2 supports: Aerosil A-175 and OX-50 ($pH_{IEP} = 3 \pm 0.1$), GT ($pH_{IEP} = 2.9$ on the background 10^{-2} M KNO_3), and a quartz plane–parallel capillary ($pH_{IEP} = 2 \pm 0.1$). Electrophoretic mobility measurements for Aerosil A-175 particles covered with titanium–oxygen nanostructures showed the following. After the first cycle of molecular layering on the preliminarily dehydrated surface at $\Theta = 0.1$, the isoelectric point of the modified SiO_2 surface shifts appreciably, by 0.4 pH units, to the alkaline region, and a positive region of the ζ potential appears. As Θ is increased to 0.5, the isoelectric point changes to $pH_{IEP} = 4.0$. The initial Aerosil A-175 surface not subjected to preliminary thermal treatment (which, in principal, allows all silanol groups to be involved in molecular layering reactions) after the first cycle of the synthesis of the Ti–oxygen layer had $pH_{IEP} = 4.4$. This value almost did not change after several successive cycles of molecular layering (from $n = 1$ to $n = 4$).

The number of cycles of the synthesis of titanium–oxygen nanolayers on the surface of GT particles was 1, 2, 6, and 11. The calculated electrokinetic potentials ζ^W of the initial and modified particles on the background of 10^{-2} M KNO_3 are represented in Fig. 3. These results were compared with data for the bulk sample of titanium oxide. The isoelectric point for

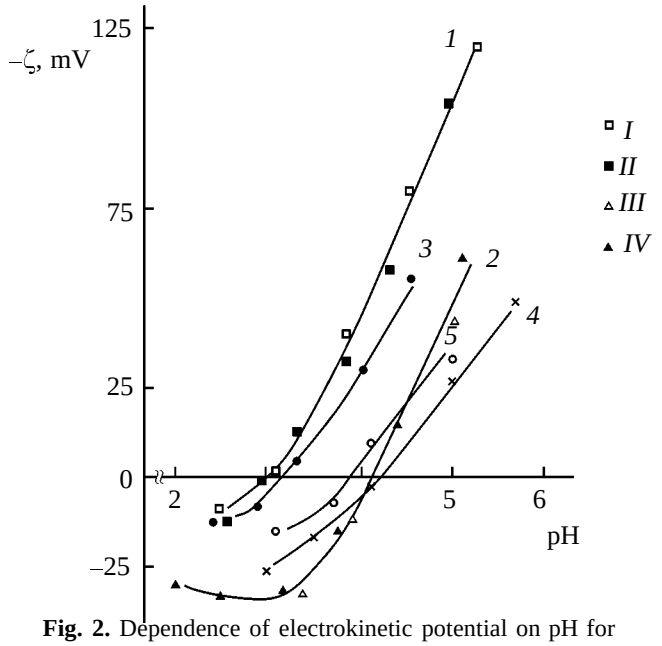

Fig. 2. Dependence of electrokinetic potential on pH for plane–parallel capillaries in HCl solutions. (*1*) Initial capillary (*I*) and $6SiO_2/SiO_2$ (*II*) and (*2*) $6TiO_2/SiO_2$ (*III*) and $16TiO_2/SiO_2$ (*IV*); on the background of 10^{-3} M NaCl: (*3*) initial capillary, (*4*) $16TiO_2/SiO_2$, and (*5*) initial surface SiO_2 + $16TiO_2/SiO_2$.

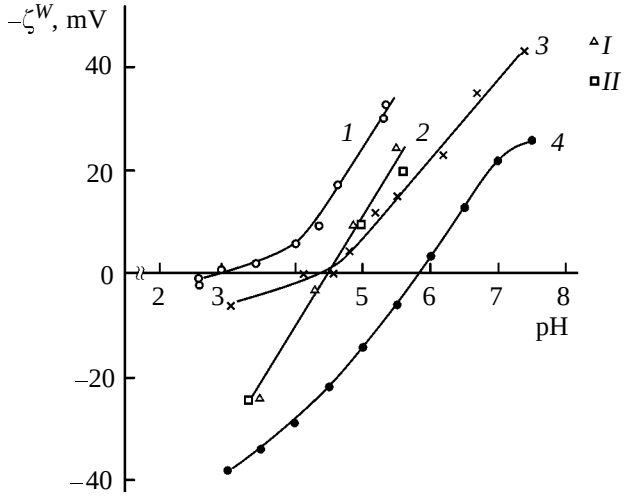

Fig. 3. Dependence of electrokinetic potential on pH on the background of 10^{-2} M KNO_3. (*1*) Monodisperse spherical SiO_2 particles; (*2*) TiO_2/SiO_2 (*I*) and $6TiO_2/SiO_2$ (*II*); (*3*) $11TiO_2/SiO_2$; and (*4*) TiO_2 on the background of 10^{-2} M NaCl.

particles covered with nanostructures is between those for the initial SiO_2 support and titanium oxide. It was also found that the isoelectric point is independent of n (at n = 1–11, $pH_{IEP} \approx 4.5$) and close to the isoelectric point for the Ti–oxygen layers on the Aerosil A-175 support at n = 1–4. Similar results were obtained for Aerosil OX-50 particles at n = 1 and 2. In this case, pH_{IEP} = 4.2 for modified particles.

Electrokinetic potential measurements for the Ti–oxygen nanostructures synthesized on the surface of a glass plane–parallel capillary at n = 6 and 16 gave pH_{IEP} = 4.2–4.3 both for HCl solutions (Fig. 2, curve *2*) and for those on the background of 10^{-3} M NaCl (Fig. 2, curve *4*). Thus, the pH_{IEP} for plane–parallel capillaries covered with titanium–oxygen nanolayers, too, differ from the isoelectric point of bulk titanium oxide. It is also seen that the electrokinetic potentials of titanium–oxygen nanostructures of different thickness are close to each other.

It was thus shown that the deposition of titanium-oxygen nanostructures changes the electrokinetic parameters of the initial silica surface, and all the supports modified by titanium–oxygen nanostructures have different electrokinetic parameters than bulk titanium oxide. On the other side, it is known from the literature [16–18, 23] that, on complete substitution of silanol groups by Ti–oxygen ones, it is sufficient to deposit four layers to create on silica surface a titanium oxide layer with an octahedrite crystallographic structure. Therefore, six or more cycles of molecular layering would inevitably form the octahedrite structure on silica surface. The fact that the isoelectric point of the SiO_2 surface covered with titanium–oxygen nanolayers differs from that of octahedrite (pH_{IEP} = 5.9) gives evidence for incomplete substitution of silanol groups, i.e. for a mosaic character of the modified surface. We also note that, in the case of Ti–oxygen nanostructures, the constancy of pH_{IEP} at increasing number of molecular layering cycles suggests that the degree of substitution of surface groups is determined in the first cycle of the reaction.

To verify the assumption that the mosaic structure of the modified surface affects the electrokinetic characteristics of the support, we measured the electrokinetic potential of a plane–parallel capillary formed by two different surfaces: the initial SiO_2 surface and the SiO_2 surface covered with the titanium–oxygen nanostructure (n = 16; Fig. 2, curve *5*). Indeed, the isoelectric point (pH_{IEP} = 3.9) is between the isoelectric points of the quartz glass and the titanium–oxygen nanostructure.

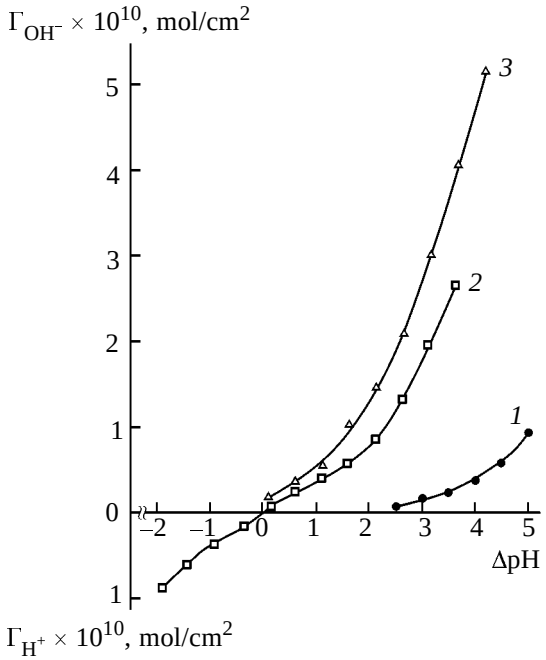

Fig. 4. Dependence of the adsorption of potential-determining ions on $\Delta pH = pH - pH_{ZCP}$ on the background of 1 M solutions of (*1*) KNO_3 and (*2*, *3*) NaCl. (*1*) SiO_2, (*2*) TiO_2, and (*3*) $11TiO_2/SiO_2$.

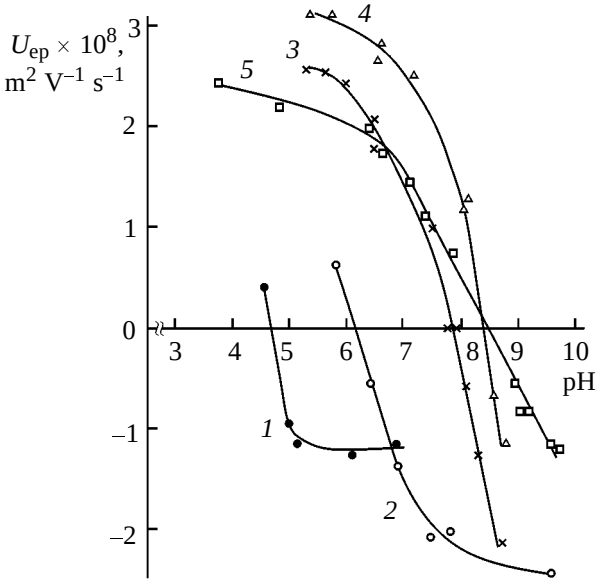

Fig. 5. Dependence of electrophoretic mobility on pH for Aerosil A-175 particles covered with Al–oxygen nanostructures on the background of 10^{-2} M NaCl: (*1*) n = 1, Θ = 0.1; (*2*) n = 1, Θ = 1; (*3*) n = 2, Θ = 1; (*4*) n = 4, Θ = 1; and (*5*) AlOOH.

Potentiometric titration is another independent method for comparison of the electrosurface characteristics of bulk oxides and ultrathin oxide layers. On the assumption that pH_{IEP} and pH_{ZPC} for titanium–oxygen nanostructures in solutions of indifferent electrolytes are equal to each other (as was observed for bulk titanium oxide), one can compare the adsorption behavior of the nanostructures and bulk silica and titanium oxide by analyzing the dependence of Γ_i on ΔpH ($\Delta pH = pH - pH_{ZPC}$).

The measured adsorptions of potential-determining ions Γ_{OH^-} on the background of 1 M NaCl for monodisperse spherical SiO_2 particles covered with the titanium–oxygen nanostructure (n = 11) are given in Fig. 4. The same figure represents the Γ_i–pH dependences for the initial substrate and for bulk titanium oxide [26]. It is of note that, potentiometric titration revealed no positive range of surface charge for SiO_2 particles modified with titanium–oxygen nanostructures, by contrast with electrokinetic measurements when a positive region of electrokinetic potential was observed. However, one should take into account that potentiometric titration is insufficiently sensitive in the acidic range (pH < 4) at low positive surface charges. Just this prevented determination of pH_{ZPC} from the Γ_i–pH dependence. The higher values of Γ_{OH^-} for modified particles as compared with bulk titanium oxide are probably related to the porosity (ion permittivity) of deposited titanium–oxygen layers. This assumption is confirmed by the results of conductivity measurements for the plane–parallel capillary covered with titanium-oxygen layers: The surface conductivity of the modified surface was higher than that of the initial one.

It is of note that the electrosurface parameters of titanium–oxygen nanostructures on silicon oxide supports, we measured in the present work, correlate with those obtained in [20] for SiO_2 particles covered by titanium oxide by deposition from solutions followed by calcination ($pH_{IEP} \approx pH_{ZPC} = 3.9 \pm 0.1$ on the background of a KNO_3 solution). The modified particles were also noted to possess high surface charges related, first of all, to the porosity of the deposited oxide layer.

System nAl$_2$O$_3$/SiO$_2$

Aluminum–oxygen nanostructures were synthesized on Aerosil A-175, OX-50, and GT particles. The results of electrophoretic measurements (Fig. 5) show that, similarly to Ti–O nanolayers on the A-175 surface, the first cycle of molecular layering at Θ = 0.1 leads to a significant shift of pH_{IEP} from its initial value to pH_{IEP} = 4.7. After the first cycle of

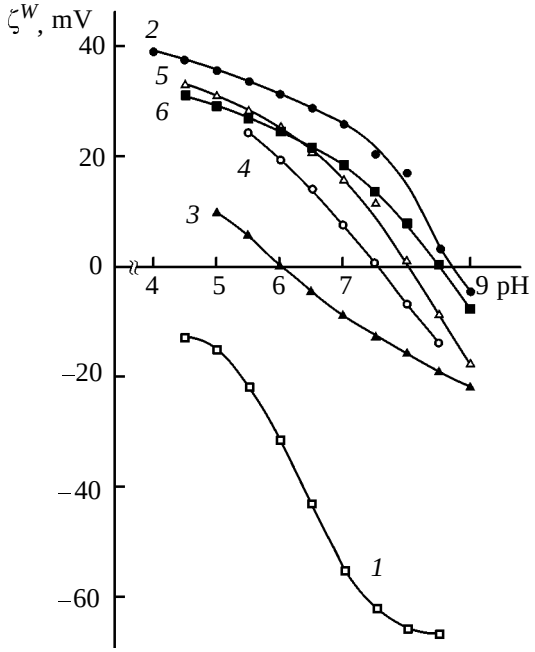

Fig. 6. Dependence of electrokinetic potential ζ^W on pH on the background of 10^{-2} M NaCl. (*1*) SiO_2 (GT), (*2*) AlOOH, (*3*) Al_2O_3/SiO_2, (*4*) $2Al_2O_3/SiO_2$, (*5*) $4Al_2O_3/SiO_2$, and (*6*) $5Al_2O_3/SiO_2$.

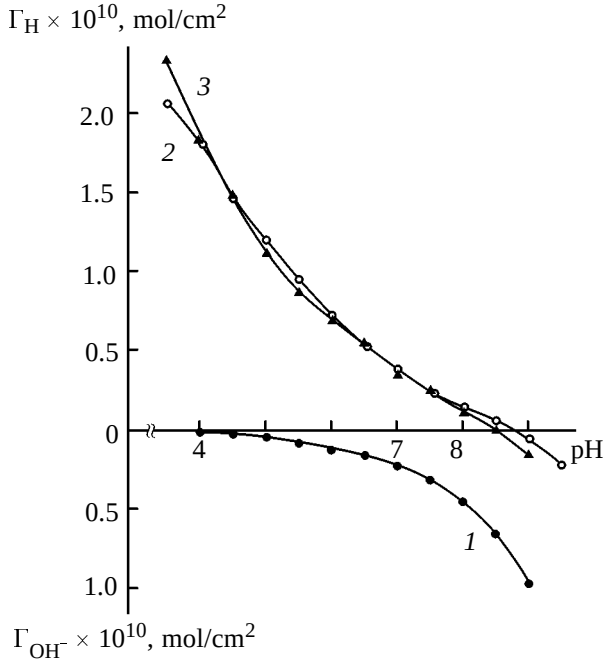

Fig. 7. Dependence of the adsorption of potential-determining ions on pH on the background of 10^{-2} M NaCl. (*1*) SiO_2 (Aerosil OX-50), (*2*) AlOOH, and (*3*) $5Al_2O_3/SiO_2$.

molecular layering on the A-175 surface not subjected to preliminary thermal treatment, pH_{IEP} increases up to 6.2. Further increase of the number of molecular layering cycles to four causes gradual shift of the isoelectric point to the alkaline region to pH_{IEP}= 8.4, which is close to the isoelectric point of bulk aluminium hydroxide (pH_{IEP}= 8.5).

The number of molecular layering cycles in the synthesis of aluminium–oxygen nanolayers on Aerosil OX-50 and GT particles was 1–5. It was found that, as the number of molecular layering cycles increases, in both cases the isoelectric point shifts to the alkaline region up to $pH_{IEP} \approx 8.5$, which practically coincides with the pH_{IEP} value for bulk (hydr)-oxyde [the ζ^W–pH dependences for the initial and modified GT particles are exemplified in Fig. 6].

The chemical analysed of Al–oxygen samples are presented in the table. As seen, the amount of aluminium oxide deposited on the SiO_2 surface increases proportionally to the number of reaction cycles and thus correlates with the gradual shift of the isoelectric point of modified samples from the pH_{IEP} of the SiO_2 surface to the pH_{IEP} of the aluminium hydroxide surface.

For the Aerosil OX-50 surface covered with five aluminum oxide layers we also measured the adsorption of potential-determining ions as a function of pH on the background of 10^{-2} M NaCl (Fig. 7). As seen from Fig. 7, the pH_{ZPC} values for modified SiO_2 particles and for AlOOH particles coincide and equal 8.6 ± 0.1. It is also noteworthy that the absorptions of potential-determining ions for the $5Al_2O_3/SiO_2$ nanostructure coincide with the Γ_i values obtained for bulk AlOOH.

The electrosurface characteristics of the nAl_2O_3/SiO_2 samples synthesized by the molecular layering method gives evidence to show that, irrespective of the kind of the silica support, the use of hydroxyl functional groups and the $AlCl_3$ vapor temperature of 200°C (note that the sublimation temperature of $AlCl_3$ is 192.5°C) yields, at n = 5, aluminum–oxygen nanostructures with electrochemical properties practically coinciding with those of bulk aluminium hydroxide.

System nSnO$_2$/AlOOH

The investigation of the electrosurface characteristics of Sn–oxygen nanolayers on the boehmite surface we started with studying the electrokinetic properties of aluminium hydroxide covered with Sn–oxygen nanolayers by reactions (1) and (2). The concentration

Chemical analyses of element(Al, Sn, Fe)–oxygen nanolayers

Al					Sn					Fe				
No.	t_{AlCl_3}, °C	support	functional group	$[Al^{3+}]$, μmol/m^2	No.	t_{SnCl_4}, °C	support	functional group	$[Sn^{4+}]$, μmol/m^2	No.	t_{FeCl_3}, °C	support	functional group	$[Fe^{3+}]$, μmol/m^2
1	200	Aerosil	OH	0.94	1	20	AlOOH	OH	0.25	1	200	SiO_2	OH	0.09
2	200	OX-50	OH	1.83	2	20		OH	0.35	2	200	"GelTech"	OH	0.15
4	200		OH	3.56	4	20		OH	0.75	4	200		OH	0.18
5	200		OH	4.21	4	20		OCH_3	0.70	4	250		OCH_3	0.31
–	–		–	–	4	100		OCH_3	9.10	4	250	??-120	OCH_3	0.17

of $SnCl_4$ in the reactor was determined by the temperature of the gooseneck with liquid chloride (20°C). The chemical analyses of Sn–oxygen nanostructures are given in the table and show that the amount of the deposited oxide increases as the number of molecular layering cycles increases from 1 to 4. It was also found that with increasing number of molecular layering cycles the isoelectric point shifts to the acidic region, attaining pH_{IEP}= 7.2 at n = 4. This value much differs both from the isoelectric point of the support (pH_{IEP} = 8.6) and from the isoelectric point of bulk SnO_2 (pH_{IEP} = 4.0±0.1). This can be related to incomplete substitution of OH functional group of the support in the course of the synthesis of Sn–oxygen nanolayers by reactions (1) and (2). Therefore, further

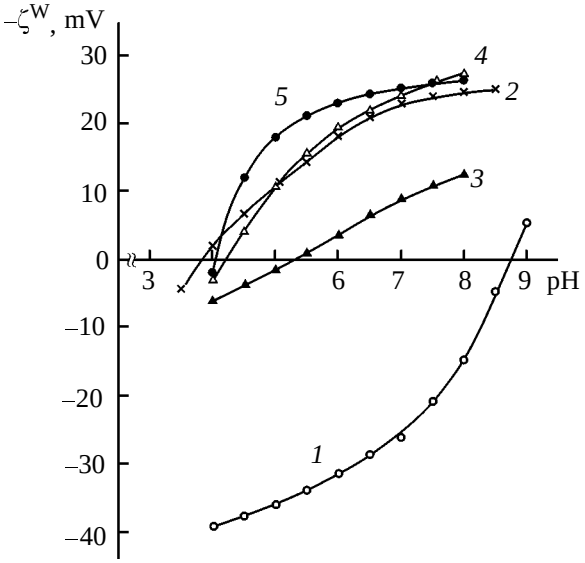

Fig. 8. Dependence of the electrokinetic potential ζ^W on pH on the background of 10^{-2} M NaCl. (*1*) AlOOH, (*2*) SnO_2, (*3*) $(4SnO_2/AlOOH)^{OH}$ (100°C), (*4*) $(4SnO_2/AlOOH)^{OCH_3}$ (100°C), and (*5*) $(4SnO_2/SnO_2)^{OCH_3}$ (100°C).

we synthesized oxide layers by reactions (3)–(6) using methoxy functional groups. However, here, too, the pH_{IEP} of the resulting SnO_2/AlOOH sample turned to be about 7.2. To verify the assumption that atmospheric oxygen affects the stability of surface methoxy groups, we studied the electrokinetic properties of the nanolayers synthesized via methoxy groups under nitrogen. In that case, the pH_{IEP} value for the $4SnO_2$/AlOOH sample was about 7.1, which practically coincides with the pH_{IEP} values for the samples synthesized under air.

To ascertain the effect of the chemical composition of the support on the characteristics of the nanostructure, the synthesis of Sn–oxygen layers via methoxy functional groups was also performed on a Silochrom C-120 support (the temperature of $SnCl_4$ was 20°C). Comparison of the ζ^W potentials obtained for bulk tin and silicon oxides and for the modified Silochrom surface $(4SnO_2/SiO_2)OCH_3$ shows that the ζ^W–pH dependences are similar to each other. However, the $|\zeta^W|$ value for Sn–oxygen layers are higher than for bulk oxides. We failed to determine isoelectric points both for SiO_2 and for $4SnO_2/SiO_2$.

To make higher the degree of substitution of surface functional groups of the support (AlOOH) in molecular layering reactions, the partial pressure of $SnCl_4$ vapor was built up by heating the gooseneck to 100°C. For preparing oxide nanolayers both OH and OCH_3 groups were used. The number of molecular layering cycles was four. The resulting pH_{IEP} values for $(4SnO_2/AlOOH)^{OH}$ and $(4SnO_2/AlOOH)^{OCH_3}$ were 5.3 and 4.2, respectively (Fig. 8). It is of note that the isoelectric point for the nanostructure $(4SnO_2/AlOOH)^{OH}$ is close to that for bulk tin oxide (4.0±0.1). Thus, increased partial pressure of $SnCl_4$ yields increased degree of substitution of functional groups, which can be related to the determining influence of reagent concentration. It should also be nated that the samples synthesized via different

functional groups exhibit different electrochemical behavior.

Compare the electrochemical characteristics of a Sn–oxygen layer deposited on a bulk oxide of the same chemical nature (SnO_2) with the properties of the surface layer of the initial bulk tin oxide we synthesized $(4SnO_2/SnO_2)^{OCH_3}$ nanostructures. The latter sample had $pH_{IEP} \approx 4.0$ value (Fig. 8, curve *5*), which is practically coincident with the pH_{IEP} value for bulk SnO2 and for the modified surface $(4SnO_2/AlOOH)^{OCH_3}$ (the temperature of $SnCl_4$ 20°C was 100°C).

For the modified samples $(4SnO_2/AlOOH)^{OCH_3}$ and $(4SnO_2/SnO_2)^{OCH_3}$ (Fig. 9) we also measured the adsorption of potential-determining ions at various pH on the background of 10^{-2} M NaCl. As seen, the pH_{ZPC} values for both the samples, as well as for bulk SnO2, practically coincide and equal 4.2 ± 0.1. We also note that the surface charges for Sn–oxygen layers deposited on various (hydr)oxide substrates, are higher than the surface charge of bulk tin oxide. Analysis of the electrosurface characteristics of Sn–oxygen nanostructures deposited on tin oxide shows that treatment of the SnO_2 surface with organic reagents causes no surface contamination, which implies complete removal of by-products from the reaction zone.

Thus, the above linking research of the electrosurface characteristics of bulk samples and samples synthesized by the molecular layering method gave evidence showing that, irrespective of the nature of the support, using methoxy groups (at the SnO_2 temperature of 100°C) makes possible preparation of Sn–oxygen nanostructures with electrochemical properties close to those of bulk oxide.

System Fe_2O_3/SiO_2

Iron–oxygen layers were synthesized on GT and Silochrom C-120 silica supports. The number of molecular layering cycles was 1–4. Furst we studied the electrokinetic properties of SiO_2 covered with Fe–oxygen nanostructures according to reactions (1) and (2) at 200°C. The chemical analyses of Fe–oxygen nanostructures are given in the table. The amount of iron deposited is seen to increase in the course of the molecular layering reaction, but to a less extent than with aluminium and tin oxide layers. Comparison of the ζ^W–pH dependences for the $n Fe_2O_3/SiO_2$ samples showed that the modified surface is negatively charged over the entire pH range studied. So we failed to determine isoelectric points for these samples.

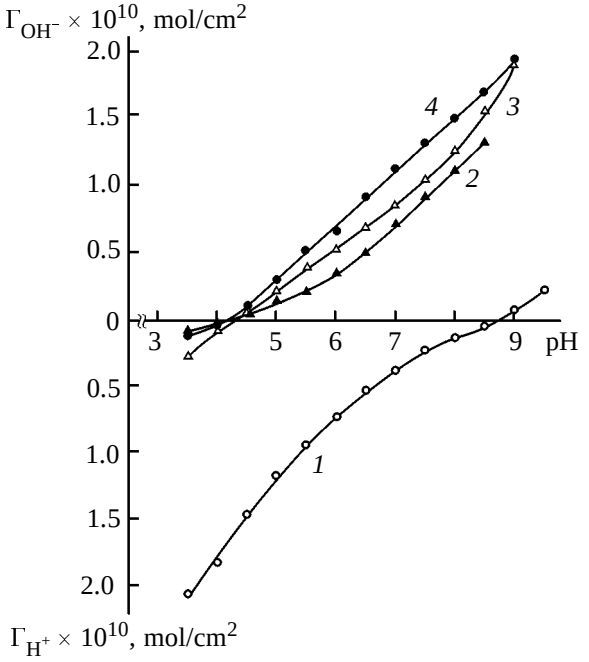

Fig. 9. Dependence of the adsorption of potential-determining ions on pH on the background of 10^{-2} M NaCl. (*1*) AlOOH, (*2*) SnO_2, (*3*) $(4SnO_2/AlOOH)^{OCH_3}$ (100°C), (*4*) $(4SnO_2/SnO_2)^{OCH_3}$ (100°C).

Iron–oxygen nanolayers on the SiO_2 surface were also synthesized via methoxy functional groups according to reactions (3)–(6). As with $nSnO_2/AlO \cdot OH^{OCH_3}$, using organic reagents with the purpose to increase the degree of substitution of functional groups without raising the temperature failed to yield a positive range of electrokinetic potentials for the resulting samples as compared with SiO_2 (Fig. 10, curve *2*). Figure 10 also displays the ζ^W–pH dependence for $(4Fe_2O_3/SiO_2)^{OCH_3}$ obtained at 250°C (Fig. 10, curve *3*). Changing reaction conditions resulted in appearance of a positive range of electrokinetic potentials ($pH_{IEP} = 3.9$), but the characteristics of the surface covered with Fe–oxygen layers are considerably different from those of bulk α-FeOOH ($pH_{IEP} = 7.2$ [29]).

Measements of the adsorption of potential-determining ions and of the electrophoretic mobility for the Silochrom C-120 surface covered with Fe–oxygen nanolayers $[(4Fe_2O_3/SiO_2)^{OCH_3}]$ gave $pH_{IEP} = pH_{ZPC} = 4.4 \times 0.1$. This value differs from the corresponding pH_{IEP} values both for the silica support and for bulk iron hydroxide (α-FeOOH). The ζ^W–pH and Γ_i–pH dependences for Fe-oxygen nanostructures are also similar to those for α-FeOOH, implying appreci-

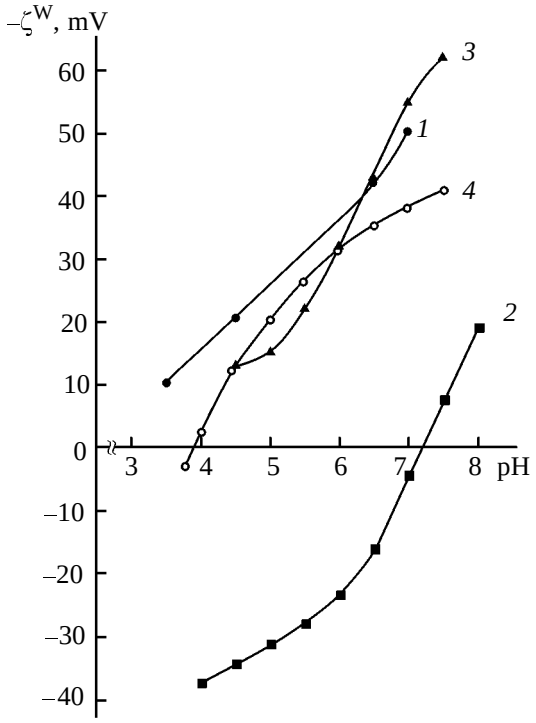

Fig. 10. Dependence of the electrokinetic potential ζ^W on pH on the background of 10^{-2} M NaCl. (*1*) SiO_2 (GT), (*2*) FeOOH, (*3*) $(Fe_2O_3/SiO_2)^{OCH_3}$, and (*4*) $(4Fe_2O_3/SiO_2)^{OCH_3}$ (250°C).

able effect of the deposited iron oxide layers on the characteristics of the modified SiO_2 surface. However, the different isoelectric point and zero-point charges for bulk oxides and for Fe–oxygen nanostructures on the SiO_2 support shows that here, too, we failed complete substitution of silanol groups of the support, in contrast with the situations observed with aluminium and tin oxide layers.

Comparison of the electrosurface characteristics of silicon, titanium, iron, tin, and aluminium (hydr)-oxides with analogous properties of element–oxygen nanostructures on silica supports allows the following conclusions:

(a) the electrosurface characteristics of a nanostructure deposited is independent of the type of the silica support;

(b) the deposition of an element–oxygen nanolayer on a support of the same chemical composition has almost no effect on the isoelectric point and the electrokinetic potential of the surface;

(c) the degree of substitution of support silanol groups by Ti–oxygen ones is determined in the first cycle of molecular layering. For all the systems investigated (n = 1–16, Θ = 1), the isoelectric point of the modified surface (pH_{IEP} = 4.2–4.5) is between the isoelectric points of silicon and titanium oxides, which suggests a mosaic structure of the surface;

(d) for Al–oxygen nanostructures, gradual substitution of support silanol groups is observed with increasing number of molecular layering cycles. The electrosurface characteristics of the nanostructure practically coincide with those of bulk aluminium hydroxide at n = 4–5;

(e) for Sn–oxygen nanostructures on the boehmite surface, we could find such molecular layering conditions that allowed an almost complete modification of the initial surface and passing from the electrosurface characteristics of AlOOH to analogous parameters of SnO_2;

(f) in the case of Fe-oxygen nanostructures on silica support, we failed to achieve complete substitution of silanol groups by Fe–oxygen ones by varying synthesis conditions;

(g) the pH values for the isoelectric and zero-charge points of an oxide covered with element–oxygen nanostructures of different chemical nature can serve as a criterion of the completeness of substitution of support surface groups in the course of the synthesis of nanostructures by molecular layering from the gas phase.

ACKNOWLEDGMENTS

The work was financially supported by the Russian Foundation for Basic Research (project no. 00-15-97 357).

REFERENCES

1. Gusev, A.I., *Nanokristallicheskie materialy: metody polucheniya i svoistva* (Nanocrystalline Materials: Preparation Methods and Properties), Ekaterinburg, 1998.
2. Sviridov, V.V. and Branitsky, G.A., *Khimicheskie problemy sozdaniya novykh materialov i tekhnologii* (Chemical Problems of Creation of New Materials and Technologies), Minsk: Belorus. Gos. Univ., 1998, pp. 293–430.
3. Van den Vlekkert, H., Bousse, L., and de Rooij, N., *J. Colloid Interface Sci.*, 1988, vol. 122, no. 2, pp. 336–345.
4. Bobrov, V.P., Krauze, C., and Tarantov, Yu.A., *Zh. Prikl. Khim.*, 1991, vol. 64, no. 3, pp. 546–551.
5. Bobrov, V.P., Bratov, A.V., and Tarantov, Yu.A., *Zh. Prikl. Khim.*, 1991, vol. 64, no. 12, pp. 2619–2629.
6. Velikova, M., Damyanov, D., and Mehadjiev, D., *Izv.*

Khim. Bolg. Akad. Nauk, 1979, vol. 12, no. 4, pp. 647–651.

7. Ermakov, Yu.I., Zakharov, V.A., and Kuznetsov, B.N., *Zakreplennye kompleksy na okisnykh nositelyakh v katalize* (Fixed Complexes on Oxide Supports in Catalysis), Novosibirsk: Nauka, 1980.
8. Hair, M.L. and Hertl, W., *J. Phys. Chem.,* 1973, vol. 77, no. 17, pp. 2070–2075.
9. Ellestad, O.H. and Blindheim, U., *J. Mol. Catal.,* 1985, vol. 33, no. 3, pp. 275–287.
10. Smirnov, V.M., Malkov, A.A., and Rachkovsky, P.P., *Zh. Prikl. Khim.,* 1992, vol. 65, no. 12, pp. 2666–2671.
11. Smirnov, V.M., Rachkovsky, P.P., and Voronkov, G.P., *Zh. Obshch. Khim.,* 1993, vol. 63, no. 2, pp. 278–282.
12. Smirnov, V.M., *Khimiya nanostruktur. Sintez, stroenie, svoistva* (Chemistry of Nanostructures. Synthesis, Structure, Properties), St. Petersburg: S.-Peterb. Gos. Univ., 1996.
13. Malygin, A.A., Malkov, A.A., and Dubrovenskii S.D., *Studies in Surface Science and Catalysis,* Amsterdam: Elsevier, 1996, vol. 99, pp. 213–233.
14. Aleskovskii, V.B., *Khimiya nadmolekulyarnykh soedinenii* (Chemistry of Supramolecular Compounds), St. Petersburg: S.-Peterb. Gos. Univ., 1996.
15. Schrijnemakers, K., Van der Voort, P., and Vansant, E.F., *Phys. Chem. Chem. Phys.,* 1999, vol. 1, pp. 2569–2572.
16. Pak, V.N., *Zh. Fiz. Khim.,* 1976, vol. 50, no. 5, pp. 1266–1268.
17. Tikhomirova, I.Yu., Nikolaev, Yu.S., Burkat, T.M., Ragulin, G.K., and Pak, V.N., *Zh. Fiz. Khim.,* 1989, vol. 63, no. 2, pp. 517–519.
18. Pak, V.N., Tikhomirova, I.Yu., Burkat, T.M., and Lobov, B.I., *Zh. Fiz. Khim.,* 1999, vol. 73, no. 11, pp. 2024–2028.
19. Vlasov, Yu., Bratov, A., Sidorova, M., and Tarantov, Yu., *Sens. Actuatorts,* 1990, vol. 1, pp. 357–360.
20. Giatti, A. and Koopal, L.K., *J. Electroanal. Chem.,* 1993, vol. 352, no. 1, pp. 107–118.
21. Rasmussen, M. and Staffan, W., *Colloids Surf.,* 1997, vol. 122, pp. 169–181.
22. Kol'tsov, S.I. and Aleskovskii, V.B., *Zh. Prikl. Khim.,* 1968, vol. 42, no. 5, pp. 1210–1214.
23. Kol'tsov, S.I., *Zh. Prikl. Khim.,* 1969, vol. 43, no. 5, pp. 1023–1028.
24. Malkov, A.A., Sosnov, E.A., Osipenkova, O.V., and Malygin, A.A., *Appl. Surf. Sci.,* 1997, vol. 108, pp. 133–139.
25. Bogdanova, N.F., Sidorova, M.P., Ermakova, L.E., and Savina, I.A., *Kolloid. Zh.,* 1997, vol. 59, no. 4, pp. 452–459.
26. Sidorova, M.P., Ermakova, L.E., Bogdanova, N.F., and Proner, M.A., *Kolloid. Zh.,* 1999, vol. 61, no. 1, pp. 108–112.
27. Ermakova, L., Sidorova, M., Bogdanova, N., and Klebanov, A., *Colloids Surf.,* 2001, vol. 192, pp. 337–348.
28. Klebanov, A.V., Bogdanova, N.F., Ermakova, L.E., Sidorova, M.P, and Osmolovskii, M.G., *Kolloid. Zh.,* 2001, vol. 63, no. 5, pp. 617–623.
29. Klebanov, A.V., Bogdanova, N.F., Ermakova, L.E., and Sidorova, M.P., *Kolloid. Zh.,* 2001, vol. 63, no. 5, pp. 624–628.
30. Wiersema, P.H., Loeb, A.L., and Overbeek, J.T.G., *J. Colloid Interface Sci.,* 1966, vol. 22, no. 1/2, p. 78.